Accelerator Requirements for HEDP
John Barnard

In order to set the requirements on an ion accelerator for heating a target to Warm Dense Matter conditions, a number of accelerator and target parameters must be understood Scaling relations between the ion energy loss rate (dE/dX), and the ion energy and mass; at least a rough understanding of the equation of state for the matter that is to be studied, and an understanding of the relation between the achievable pulse duration and focal spot on accelerator and beam parameters are needed. In this note, we try to connect some of these basic parameters to help search the extensive parameter space (including ion mass, ion energy, total charge in beam pulse, beam emittance, target thickness and density, to name a few of the parameters) and obtain a sensible set of accelerator and beam parameters which can achieve interesting Warm Dense Matter conditions.

We first examine dE/dX, where E is the ion energy and $X \equiv \int \rho \, dz$ is the integrated range of the ion. This quantity has been displayed graphically for a number of different ions, in ref [1], and scaling to other target materials is also given.

For heating solid aluminum (at room temperature) over a range of ion mass from 4 amu (Helium) to 126 amu (Iodine), the energy loss at the peak of the dE/dX curve (dE/dX_{max}) may be parameterized approximately as:

$$(1/Z^2)dE/dX_{max} \approx 1.09 \text{ (MeVcm}^2\text{/mg)} \, A^{-0.82} \tag{1}$$

where Z and A are the ion nuclear charge and atomic mass, respectively. Expressing $dE/dX_{\max}$ as a function of A only yields:

$$dE/dX_{max} \approx 0.35 \text{ (MeVcm}^2\text{/mg)} \, A^{1.07}. \tag{2}$$

Thus, the peak energy loss rate increases (nearly linearly) with ion atomic mass.

Similarly, the energy at the peak increases with ion nearly quadratically with A:

$$E \text{ (at } dE/dX_{max}) \approx 0.052 \text{ MeV } A^{1.803} \, . \tag{3}$$

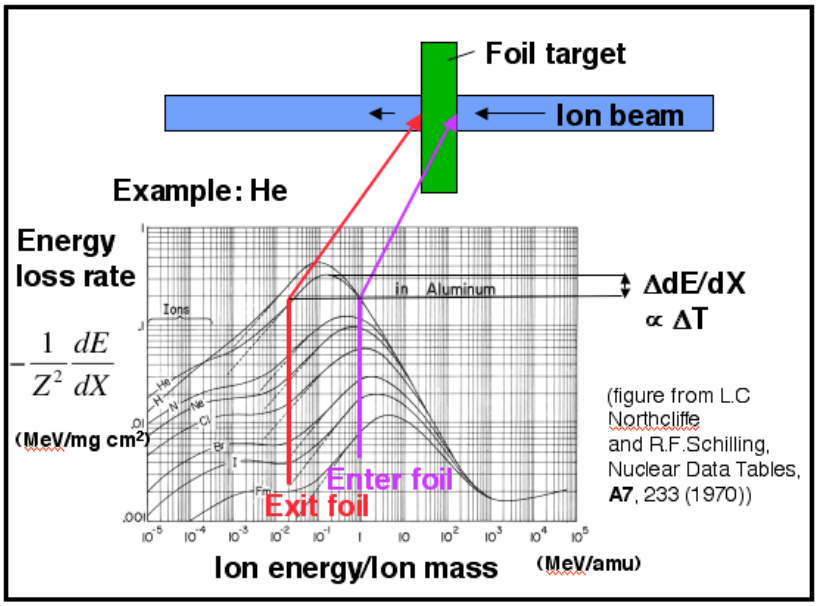

Figure 1. Temperature variations in an ion-beam heated foil can be minimized by choosing an ion and energy such that the peak in dE/dX occurs in the center of the foil (ref. [2]).

Target uniformity is another important consideration. In ref. [2] it was pointed out that target temperature uniformity can be maximized in simple planar targets if the particle energy reaches the maximum in the energy loss rate *dE/dX* when the particle has reached the center of the foil (see figure 1). For any specified fractional deviation in target temperature (assuming the energy is deposited in a time short so that no hydrodynamic, radiative, or other cooling has occurred) one can determine the energy at which the ion must enter and exit the foil. From the *dE/dX* curves of ref. [1] we find that for the entrance and exit energies to have a 5% lower energy loss rate relative to the peak in *dE/dX*, $\Delta E/E \approx 1.2$, where ΔE is the difference in ion energy between entering and exiting the foil, and E is the energy at which *dE/dX* is maximum. Note the large (>1) fractional range in energy relative to peak energy is expected for a broad peak in a log-log representation. The spatial width of the foil Z, for a 5% temperature non-uniformity is then given by:

$$Z = \Delta E/(\rho\, dE/dX) \approx 0.77\mu\quad A^{0.733}(\rho_{al}/\rho) \tag{4}$$

Here we have used ρ_{al}=2.7 g/cm^3 to convert the range into a physical distance. So by using materials of low density such as metallic foams, for example, the width of the foil can be large, which can be advantageous as will be shown. The total energy density U, calculated from the total energy deposited over the course of the pulse and neglecting losses is thus:

$$U = N_{ions}E/\pi r^2 Z = 3.7 \text{ x } 10^9\ (\text{J/m}^3)(N_{ions}/10^{12})(1\text{ mm}/r)^2\ (\rho/\rho_{al})\ A^{1.07} \tag{5}$$

Here N_{ions} is the number of ions in the pulse, and r is the equivalent radius of the focal spot, defined such that the beam is assumed to have uniform density within r, and has zero intensity outside of r. So to achieve high energy density, large particle number, small spot radius, and higher target densities must be attained. In addition, to realize the

energy density given by eq. (5), the hydrodynamic expansion timescale Z/c_s must be much shorter than the pulse duration Δt.

Hydrodynamic disassembly time:

The sound speed c_s is given by $c_s = (\gamma P/\rho)^{1/2} = (\gamma[\gamma\text{-}1]U/\rho)^{1/2}$. Here γ is the ratio of specific heats, P is the pressure and ρ is the mass density. For estimating purposes, we take γ to be 5/3, although more refined estimates below will relax this assumption. For a "shock tube," that at a finite longitudinal distance z, has a discontinuous drop to zero pressure at some initial time, an analytical solution exists (ref. [3]; see fig.2) in which a rarefaction wave propagates inward at speed c_s, and a plasma front flows outward at 2 c_s. For the case of isochoric heating, when the pulse duration $\Delta t << \Delta z/ c_s$, where Δz is the width of the foil, the dynamics will be the same as the shock tube solution. For times $\Delta t <\sim \Delta z/ c_s$, we expect that, since the sound speed is increasing over the course of the pulse, the position of the rarefaction wave z_r will be somewhat less than would be expected if calculated on the basis of the final heated plasma:

$$z_r = \int_0^t c_s dt = \frac{2}{3} c_{s*} \Delta t \left(\frac{t}{\Delta t} \right)^{3/2} . \qquad (6)$$

Here $c_{s*} = c_s(T_*)$ and we assume $\frac{T}{T_*} = \frac{t}{\Delta t}$, where T_* is the temperature achieved at the end of the ion pulse; we also assume $c_s \propto T^{1/2}$.

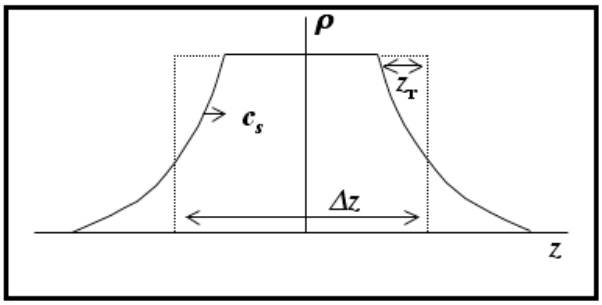

Figure 2. Schematic representation of rarefaction wave propagating inward at sound speed c_s, and plasma front moving outward at speed c_s. As material is heated over course of pulse c_s increases. The original density distribution of the foil is indicated by dotted line, and location of the rarefaction wave by z_r.

We envision isochorically heating a target foil, and taking measurements with various optical or beam diagnostics. If our diagnostic is unable to resolve a volume smaller than the volume heated by the ion beam, and if we want to distinguish equations of state with 5% accuracy, then the sample volume cannot consist mostly of blow off material (i.e. material that is part of the rarefaction wave). If we demand that the blow off material is less than 5% of the total mass, that implies $2z_r/\Delta z < 0.05$, or

$$\Delta t < 3\Delta z/(80\, c_{s*}). \qquad (7)$$

If on the other hand, the diagnostic has resolution z_{min} such that it can sample a fraction of the target ($z_{min} < \Delta z$), then, as long as the central part of the target has not been

"contaminated" by the rarefaction wave, useful data can be obtained by just observing the central (heated) part of the foil. In this latter case, the pulse duration must satisfy

$$\Delta t < 3(\Delta z - \Delta z_{min})/(4\, c_{s*}). \quad (8)$$

If $\Delta z >> \Delta z_{min}$, this can be a significantly longer time, but in any case, the longer of the two timescales above (eq. 7 and eq. 8) should be taken. For our examples to be discussed below, we have used Δz_{min} to be 40 μ, which may be achievable using a K-α diagnostic generated by a short pulse laser.

In order to calculate more accurately the sound speed, one needs to understand the response of the target to the energy deposited by the ion beam. In particular, the pressure and temperature will depend on the ionization state of the plasma. For our estimating purposes, we use a model developed by Zeldovich and Raizer and summarized in ref. [4]. The basic idea of the model is to calculate the average ionization state Z^* by approximately solving the Saha equation and accounting for the ionization energy of each ion in the energy density U (where $U = (3/2)nkT + Q(Z^*)\rho/Am_h$), and to include contributions to the pressure P (where $P = nkT = kT\,(Z^* + 1)\,\rho/Am_h$) from the electrons and partially ionized target atoms. Here $Q(Z^*) = \Sigma_{i=1}^{Z^*} I_i$, where I_i is the (known) ionization energy of the i^{th} level of the target material, n is the total number density of ions, atoms, and electrons, and ρ is the mass density. Other more detailed equation of state models, including degenerate effects, correlation effects, and more exact treatment of the Saha equation, may have an impact on various transport and thermodynamic properties. These details are not to be minimized; after all that is why there is an experimental interest in this regime. For our purposes, however, the Zelodovich-Raizer equation of state allows approximate calculation of Z^* (see fig. 9), T, and the coupling parameter Γ_{ii}.

A second model for equation of state uses the Thomas Fermi model for calculating the distribution of electrons within an atom (see ref. [5], and reference therein for a description). Results of both models for the mean ionization state Z^* are displayed in Figure 3.

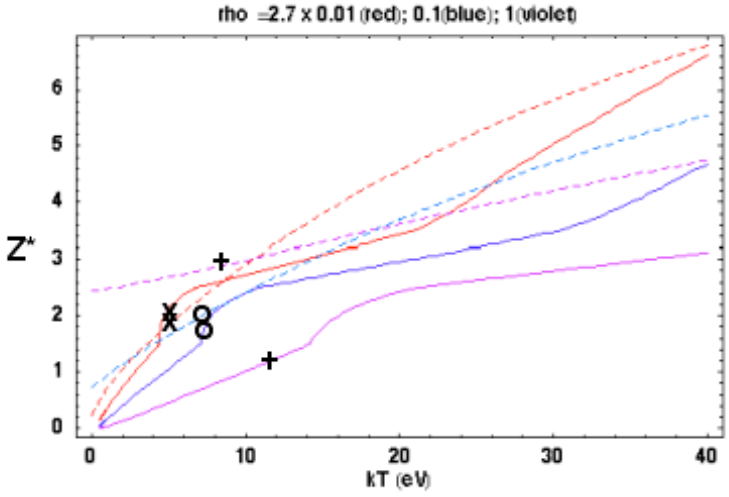

Figure 3. Calculation of ionization state, as a function of temperature for three different densities

(0.01:red, 0.10: blue, 1.00:violet) time solid density Al, using Zeldovich-Raizer equation of state(dashed) or Thomas Fermi model (solid). The x,o, and + would correspond to the conditions of reached in accelerator described by the central column of each of the 1%, 10%, and 100% solid density cases in Table 1.

Examples of accelerator requirements:

Using the model described in the previous section for ion beam stopping, the time scale for hydrodynamic expansion and the equation of state we are able to make estimates of the required beam parameters for exploring the Warm Dense Matter regime. Tables 1 and 2 give examples of requirements for two different ion energy and mass, Neon^{+1} (A=20.17) at foil entrance energy (E_{max}) of 19 MeV, and Chlorine^{+1} (A=35.453) at E_{max}=52.4 MeV. The energy at the center of the foil (E_{center}) and the energy at the exit of the foil (E_{min}) are listed in the captions to the tables. For each ion, three different mass densities of Aluminum target are given: Solid density (2.7 g/cm^3) and 10% and 1% of solid, which can be produced by making an aluminum "foam." In turn for each target density, three target temperatures are shown. Both tables are based on a minimum diagnosable length scale Z_{min} of 40 μ. It is clear from the tables that solid density, although resulting in the highest energy density, requires vary short pulse durations, because the foil width is smaller than Z_{min} and so only a small rarefaction wave propagation distance is allowed. But for the 1% and 10% cases, the foil is larger than Z_{min}, so that the rarefaction wave propagation distance can be 10's or 100's of microns, with concomitantly longer pulse duration times. In all cases the plasma temperature is in the few to tens of eV, and the required number of particles is in the order of 10^{12} to 10^{13} particles, for equivalent focal spot radii of 1 mm.

ρ(g/cm^3)(%solid)	0.027 (1%)			0.27 (10%)			2.7 (100%)		
Foil length (μ)	480			48			4.8		
kT (eV)	3.1	4.8	15	4.2	7.3	18	5.9	12	22
Z*	1.1	2.1	2.7	0.56	1.7	2.6	0.56	1.2	2.5
$\Gamma_{ii}=Z^{*2}e^2n_i^{1/3}/kT$	0.45	1.1	0.95	0.30	0.63	1.4	0.30	0.70	1.6
$N_{ions}/(r_{spot}/1mm)^2/10^{12}$	1	3	10	1	3	10	1	3	10
Δt (ns)	84	48	27	3.8	2.2	1.2	0.04	0.03	.014
U (J/m^3)/10^{11}	.015	.045	0.15	0.15	0.45	1.5	1.5	4.5	15

Table 1. Neon beam: Z=10, A=20.17, E_{min}=7.7 MeV, E_{center}=12.1 MeV, E_{max}=20.1 MeV, and Δz_{min}=40 μ

$\rho(g/cm^3)$(%solid)	0.027 (1%)			0.27 (10%)			2.7 (100%)		
Foil length (μ)	1050			105			10.5		
kT (eV)	3.8	6.5	20	5.2	8.5	25	7.6	14	31
Z*	1.3	2.5	3.5	1.1	2.2	3.2	0.75	1.5	2.8
$\Gamma_{ii}=Z^{*2}e^2n_i^{1/3}/kT$	0.45	1.1	0.71	0.61	1.5	1.1	0.42	0.77	1.5
$N_{ions}/(r_{spot}/1mm)^2/10^{12}$	1	3	10	1	3	10	1	3	10
Δt (ns)	96	56	30	6.2	3.5	2.0	0.050	0.028	.012
U $(J/m^3)/10^{11}$	.022	.065	0.22	0.22	0.65	2.2	2.2	6.5	22

Table 2. Chlorine beam: Z=17, A=35.453, E_{min}=21.1 MeV, E_{center}=48.8 MeV, E_{max}=68.5 MeV, and Δz_{min}=40 μ.

Beam Ion	Z	A (amu)	Energy at Bragg Peak (MeV)	dE/dX at Bragg Peak (MeV-mg/cm2)	Foil Entrance Energy (app) (MeV)	Delta z for 5% T variation (10% solid Al) (microns)	Beam Energy for 10 eV (J/mm2)	t_hydro= delta z/(2 cs) at 10 eV (ns)	Beam Power per sq. mm (GW/mm2)	Beam current for 1 mm diameter spot (A)
Li	3	6.94	1.6	2.68	2.4	22.1	3.3	0.5	6.1	1990.6
Na	11	22.99	15.9	11	23.9	53.5	8.0	1.3	6.1	200.3
K	19	39.10	45.6	18.6	68.4	90.8	13.6	2.2	6.1	69.8
Rb	37	85.47	158.0	39.1	237.0	149.7	22.4	3.7	6.1	20.2
Cs	55	132.91	304.0	59.2	456.0	190.2	28.5	4.7	6.1	10.5

Tabel 3. Parameters for five different ion beam species such the central temperature of a 10% solid density Aluminum foil reaches 10 eV,

Tolerance on Velocity Spread:

Several different types of accelerators are being considered to produce the very short (<~ ns) pulses required for HEDP studies. But one common thread in all of the approaches, has been the need to invoke neutralized drift compression, to overcome the limit imposed by space-charge. Neutralized drift compression is a departure from the more traditional approach of non-neutral drift compression that allows the longitudinal space charge to cause the beam velocity to "stagnate," thereby removing the velocity tilt, just as the beam is passing through the final focusing magnets, thus minimizing any potential chromatic aberrations that arise in the final focusing process. Using neutralized drift compressions achieves shorter pulses, but the various longitudinal parts of the beam that have different longitudinal velocities maintain those velocities through to the end, including the final focus. So, not only do the final focusing optics have to be tolerant of velocity spread, but target heating uniformity must be maintained as different parts of the beam (with different longitudinal velocities) will have different stopping powers (dE/dX) and which in principal lead to a temperature variation larger than that of a single particle near the Bragg peak.

To investigate the effect of velocity spread we integrated the dE/dX curves of ref. [1]. As an example we investigated the evolution of a Ne ion beam propagating through 4.8 μ foil of aluminum (see figs. 4 and 5). To represent the effect of a velocity spread we chose a number of different ion energies and averaged the energy loss rate at each point

in the foil (corresponding to a energy distribution that is uniform between a lower and upper energy cutoff), and then calculated the maximum change in energy loss rate and normalized to the average energy loss rate in the foil (= $\Delta T/T$). In the 4.8 μ foil case, for Neon with energy centered about 20 MeV and with zero energy spread, there was a 5.4% fractional spread in dE/dX through the foil. (So $\Delta T/T$=0.054 for this example, and is defined as the difference between the maximum and minimum energy loss rate divided by the average energy loss rate). As we increased the energy spread of the He beam, the calculated $\Delta T/T$ did not significantly increase until the velocity spread $\Delta v_{spread}/v=(1/2)\Delta E_{spread}/E$ is of order the fractional energy change of a single particle through the foil $\Delta E_{single\_particle}/E$. Here ΔE_{spread} is the half width of the uniform particle distribution in energy and Δv_{spread} is the corresponding velocity spread. The general conclusion, would appear to be that if $\Delta E_{spread} <\sim \Delta E_{single\_particle}$ then there is no appreciable degradation of the uniformity. On the other hand, there does not appear to be a significant advantage in a small but finite energy spread. Both statements need to be verified over a broad range of foil thickness and particle energy spreads, and the dependence on particle distribution function needs to be explored. If confirmed the temperature uniformity variations in the target may not be the most severe limitation to the allowed energy spread from velocity tilt, but more likely final optics considerations.

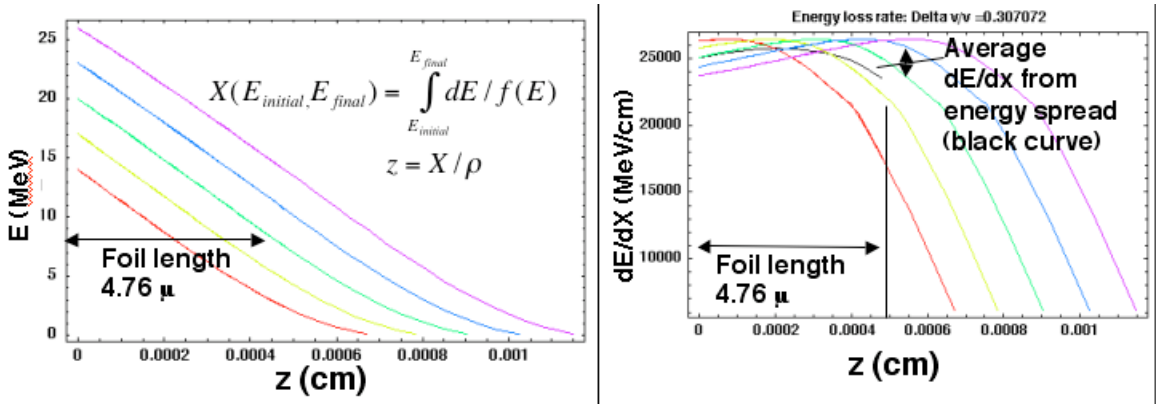

Figure 4. Energy vs. distance and dE/dX vs distance, for a Ne ion propagating in cold aluminum, for five different energies ranging from 14 to 26 MeV. The black curve in the right hand figure is the average of the five colored curves and represents the total average energy loss rate for an ion distribution function that is uniform in energy.

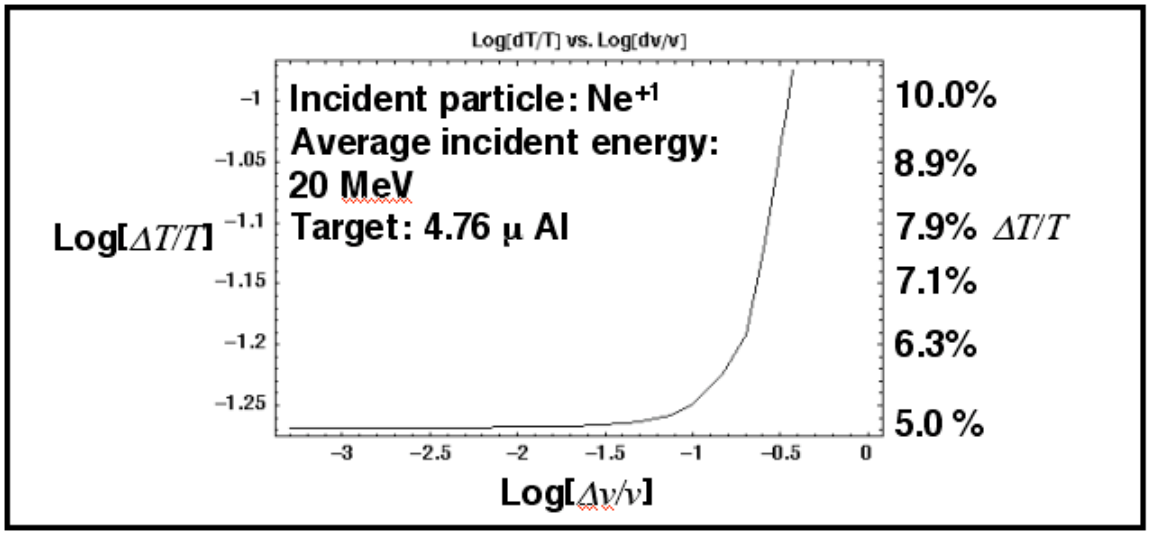

Figure 5. Temperature uniformity vs. velocity spread, for a Ne beam with central energy 20 MeV, propagating through a 4.8 μ cold aluminum foil.

Not only do HEDP experiments require uniform deposition but they also require high intensity, which means both short pulse and small beam radius. We may make simple estimates for the contribution to the spot size from chromatic effects (i.e. for the effects of a velocity spread) from a number of optical systems. For example, for a "thick" solenoidal lens in which a beam enters a solenoid with zero convergence angle and focuses to a spot within the solenoid, it can be shown to have a radius from emittance and chromatic effects r_{spot} to be approximately:

$$r^2_{spot} \approx (\pi r_0 /2)^2 (\Delta v_{spread}/v)^2 + (2\varepsilon f/\pi r_0)^2 \qquad (9)$$

where r_0 is the radius of the beam at the entrance to the solenoid, f is the focal length, i.e., the distance from the entrance of the solenoid to the focal spot, and ε is the beam emittance. The quantity r_{spot} is minimum when $r_0^2=(2/\pi)\varepsilon f /(\Delta v_{spread}/v)$ and has the value

$$r_{spot}^{\ 2} = 2\varepsilon f \, \Delta v_{spread}/v \qquad (10)$$

At minimum pulse duration the velocity tilt is converted to a velocity spread, so achieving high beam intensity will limit the velocity tilt. A system which is less sensitive to velocity tilt has also been proposed, such as the adiabatic plasma lens, but the dynamic range of these types of lens are generally limited to a reduction in spot size to a factor of around 2 or less, so these will most likely be used as a final "after burner" optic, with the bulk of the focusing being carried out by a conventional, solenoid optic, for which equations (9) and (10) provide limits.

It is apparent from equation (10) that a large velocity spread has deleterious effects in the focusing. Thus a larger velocity tilt will allow a shorter pulse but will yield a large overall spot. But if the longitudinal emittance is small, a larger velocity tilt is not needed to achieve the short pulse duration. Thus one is in obtaining a small spot there are tradeoffs that can be made between longitudinal and transverse emittance, which can be made if one is easier to obtain than the other. This may be made more explicit by

expressing equation (10) in terms of the transverse and longitudinal normalized emittances:

$$r_{spot}^{\ 2} = \varepsilon_{nx}\varepsilon_{nz} f/(\sqrt{3}\beta^3 c\tau) \qquad (11)$$

Here ε_{nx} is the normalized x emittance (= $4\beta(\langle x^2\rangle\langle x'^2\rangle\text{-}\langle xx'\rangle^2)^{1/2}$) and ε_{nz} is the normalized z (longitudinal) emittance (= $2\sqrt{3}\beta(\langle z^2\rangle\langle z'^2\rangle\text{-}\langle zz'\rangle^2)^{1/2}$), f is the final focal length, β is the final velocity in units of c and τ is the final pulse duration. Prime indicates derivative with respect to the path length s, and non-relativistic velocities are assumed. Table 4 lists a number of parameters for possible 23 MeV Na beams, with final pulse duration τ of 1 ns, total charge of 0.1 mC, and final spot radius of 1 mm. The table illustrates some of the tradeoffs that can be made involving pulse duration before drift compression, velocity tilt and requirement on longitudinal and transverse emittance. It is apparent (and obvious) that the larger compression required during final neutralized drift compression the more constrained the normalized emittance will be.

Pulse duration (before drift compression) (ns)	Velocity tilt (Head to tail) dv/v_tilt	Maximum rms velocity spread dp/p_rms (befor drift comp)	Maximum emittance unnormalized 4 rms (mm-mrad)	Maximum normalized emittance 4 rms (mm-mrad)	Beam radius at solenoid entrance Ro (m)	Neutralized Drift length (m)	Maximum rms velocity spread dp/p_rms (at injector)	Normalized Long. Emittance (m-rad)
20	0.05	7.22E-04	49.5	2.3	0.031	5.34	1.98E-03	3.29E-05
20	0.1	1.44E-03	24.7	1.2	0.016	2.67	3.97E-03	6.58E-05
20	0.2	2.89E-03	12.4	0.6	0.008	1.34	7.93E-03	1.32E-04
50	0.05	2.89E-04	49.5	2.3	0.031	13.77	1.98E-03	3.29E-05
50	0.1	5.77E-04	24.7	1.2	0.016	6.89	3.97E-03	6.58E-05
50	0.2	1.15E-03	12.4	0.6	0.008	3.44	7.93E-03	1.32E-04
100	0.05	1.44E-04	49.5	2.3	0.031	27.83	1.98E-03	3.29E-05
100	0.1	2.89E-04	24.7	1.2	0.016	13.91	3.97E-03	6.58E-05
100	0.2	5.77E-04	12.4	0.6	0.008	6.96	7.93E-03	1.32E-04
250	0.05	5.77E-05	49.5	2.3	0.031	69.99	1.98E-03	3.29E-05
250	0.1	1.15E-04	24.7	1.2	0.016	35.00	3.97E-03	6.58E-05
250	0.2	2.31E-04	12.4	0.6	0.008	17.50	7.93E-03	1.32E-04
250	1	1.15E-03	2.5	0.1	0.002	3.50	3.97E-02	6.58E-04

Table 4. Comparison of requirements on a 23 MeV Na beam with final pulse duration of 1 ns, and final focal spot radius of 1 mm, assuming neutralized drift compression and solenoidal final focus, satisfying equations (9) and (11). The injected beam has energy 1 MeV and pulse duration 171 ns.

References

1. I.C. Northcliffe and R. F. Schilling, "Range and Stopping Power Tables for Heavy Ions," Nuclear Data Tables, **A7** 233-463 (1970).
2. L. R. Grisham, *Moderate Energy Ions for High Energy Density Physics Experiments,* Physics of Plasmas, **11**, 5727 (2004).
3. L.D. Landau and E.M. Lifshitz, Fluid Mechanics, [Pergamon Press, Oxford], Chapter 10, Section 92, problem 2. (1959).
4. R. J. Harrach and F.J. Rogers, J. Appl. Phys. **52**, 5592 (1981).
5. S. Atzeni and J. Meyer-ter-Vehn, "The Physics of Inertail Fusion," [Clarendon Press, Oxford], (2004).